Imaging the Rivera and Cocos Plates Shape in Western Mexico from Local Seismicity Studies

Francisco J. Núñez-Cornú*[1], Carlos Suárez-Plascencia[1], and Diana Núñez[1,2]

Abstract

The geometry of the Rivera and Cocos plates subduction below the North American plate has been studied using a total of 5337 hypocenters located in the region of Nayarit, Jalisco, Colima, and Michoacán states in western Mexico. Our results show that seismic features of the subduction at Jalisco block (JB), Colima rift zone (CRZ), and Michoacán block are well differentiated. Our study supports the hypothesis that the Jalisco subduction zone is composed of two fore-arc blocks, Banderas and Jalisco fore-arc blocks, separated by the Ipala canyon (Bandy fault). In this region, the crustal thickness of the JB is ~30 km, whereas the Michoacán block is 35 km thick. We identified four crustal blocks along the coast in the JB from shallow seismicity data. Moreover, we found that the Rivera plate is segmented into three sections with different sizes and geometries evidenced by deep seismicity data. There is no evidence of a slab below the CRZ due to seismicity being scarce, except on the coast and the Colima volcano area where deep earthquakes (>70 km) are observed, which could be related to magmatic processes. The seismicity of the subduction process of the Cocos plate appears homogeneous, except for a seismic cluster at the mouth of Coalcomán River, where the epicentral area of the 1973 and 2021 earthquakes is located. Our results show that the Cocos plate is subducting with an inclination of 24°–30° and is slightly bent in a northwesterly direction. Therefore, our study suggests that current seismotectonic models of the region should be revised.

Cite this article as Núñez-Cornú, F. J., C. Suárez-Plascencia, and D. Núñez (2024). Imaging the Rivera and Cocos Plates Shape in Western Mexico from Local Seismicity Studies, *Seismol. Res. Lett.* **XX**, 1–17, doi: 10.1785/0220230323.

Introduction

The states of Nayarit, Jalisco, Colima, and Michoacán are included in one of the most seismically active regions of Mexico. Since 1544, earthquakes have been documented (Núñez-Cornú, 2011), and strong events have occurred along the coast, such as those of 3 June 1932 (M_s 8.2) and 18 June 1932 (M_s 7.8; Fig. 1). With the hypothesis that the Rivera plate (RP) and its slab have a simple geometry, the average recurrence time for large earthquakes obtained by comparison with the return periods of similar 1932 earthquake events in the Jalisco block (JB) was about 77 yr (Singh *et al.*, 1985). Another earthquake with M_s 8.0 (Fig. 1) took place offshore of Jalisco in October 1995, with its epicenter in the southern half of the 1932 earthquake zone (Pacheco *et al.*, 1997; Escobedo *et al.*, 1998). Other tectonic features also produce devastating earthquakes: one occurred near Islas Marías archipelago on 3 December 1948, causing extensive damage to the María Madre Island (Fig. 1). A nonsubduction earthquake of M_w 7.4 occurred on 22 January 2003, within the continental shelf near the Colima rift zone (CRZ; Núñez-Cornú *et al.*, 2004, 2010). It has been identified in the coastal region of Jalisco–Colima–Michoacan that at least 15 earthquakes with $\mathbf{M} > 7.0$ have occurred in the last 460 yr (Fig. 1, Table 1).

Tectonic Setting

The interaction of the North American (NOAM), RP, and Cocos (CP) tectonic plates (DeMets and Stein, 1990) generates a notable geotectonic complexity in western Mexico (Fig. 1), which still is poorly understood. The JB—an independent tectonic unit of North American plate (Luhr *et al.*, 1985; DeMets and Stein, 1990, Frey *et al.*, 2007) is bounded by the CRZ on the east; it borders the Pacific coast and bounds to the north with the Tepic-Zacoalco rift zone with a northwest–southeast tendency. The connection between the northwest margin of JB and the continent is not well defined. This boundary has been associated with the Islas Marías escarpment (Fig. 1); furthermore, there is no clear evidence of an active subduction zone north of Islas Marías archipelago (from north to south named María Madre, María Magdalena, and María Cleofas) (Dañobeitia *et al.*, 2016; Núñez-Cornú *et al.*, 2016; Madrigal *et al.*, 2021). On the other

1. C.A. Sismología y Volcanología de Occidente (SisVOc), CUCSH, Universidad de Guadalajara, Puerto Vallarta, Mexico, https://orcid.org/0000-0003-1515-1349 (FJN-C); https://orcid.org/0000-0003-2494-6098 (CS-P); 2. Dpto. Física de la Tierra y Astrofísica, Universidad Complutense de Madrid, Madrid, Spain

*Corresponding author: pacornu77@gmail.com

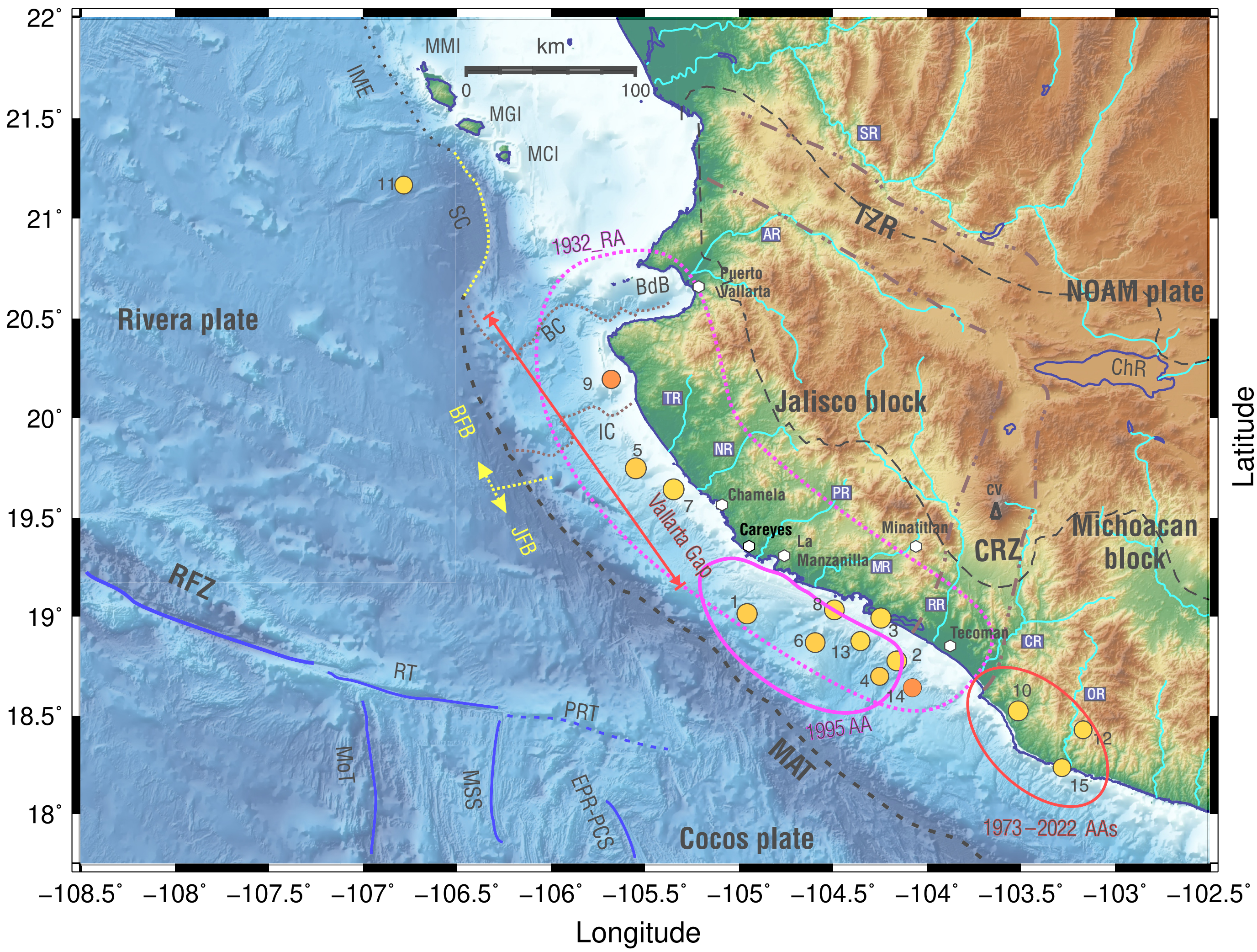

hand, the Rivera subducted plate is delineated by seismicity at south of María Cleofas Island (MCI) (Tinoco-Villa, 2015; Núñez-Cornú *et al.*, 2016; Carrillo-de la Cruz, *et al.*, 2019; Núñez *et al.*, 2021).

It is well established (e.g., Fitch, 1972; Jarrard, 1986; Beck, 1991; McCaffrey *et al.*, 2000) that the strain produced by oblique convergence is commonly partitioned into a trench-normal strain and a trench-parallel strain.

Although there are important differences between the various models proposed for the relative motion between the RP and NOAM (e.g., DeMets and Stein, 1990; Kostoglodov and Bandy, 1995), most of the models predict that the convergence direction between these two plates is increasingly oblique in a counterclockwise sense relative to the trench-normal direction, because one goes northwestward along the trench (e.g., Kostoglodov and Bandy, 1995).

Because of the oblique convergence between the RP and NOAM, the Mesoamerican Trench (MAT) curves sharply to the north at 20° N and also increases markedly the obliquity of subduction at 20° N; the fore-arc area between 19.82° and 20.16° N is subjected to greater trench-parallel extension than areas to the north or south. Urías-Espinosa *et al.* (2016) proposed that the fore-arc area of the Jalisco subduction zone has been fractured, forming at least two crustal blocks. Extensional structures are generated perpendicular to the trench that marks the limit between the fore-arc's main and independent blocks. This structure corresponds to the Ipala

Figure 1. Tectonic framework of the western Mexican region. Rupture area proposed for 1932 earthquakes (1932 RA); 1995 earthquake aftershock area (1995 AA; Pacheco *et al.*, 1997). 1973 and 2022 earthquakes aftershocks areas (1973–2022 AAs; Singh *et al.*, 2023). Abbreviations: BC, Banderas canyon (dotted line); BdB, Bahía de Banderas; BFB, Bahía de Banderas fore-arc block; JFB, Jalisco fore-arc block (Urías-Espinosa *et al.*, 2016); MAT, Middle American trench (black dashed line); MoT, Moctezuma trough; MSS, Moctezuma spreading segment; PRT, Paleo Rivera transform fault (blue dashed line; after Núñez-Cornú *et al.*, 2018); RT, Rivera transform fault (blue line); SC, Sierra de Cleofas (yellow dotted line); TZR, Tepic-Zacoalco rift zone. Rivers are indicated by blue squares: AR, Ameca; CR, Cohuayana; MR, Mascota; NR, San Nicolás; OR, Coalcomán; PR, Purificación; RR, Armería; SR, Santiago; and TR, Tomatlán. The yellow circles mark the epicenters of the earthquakes in Table 1. (Modified from Marín-Mesa *et al.*, 2019). The color version of this figure is available only in the electronic edition.

TABLE 1
Historical Earthquakes with M > 7.0 with Epicenter along the Coast

Number	Date (yyyy/mm/dd) Time (hh:mm)
1	1563/05/12
2	1771/03/10 08:00
3	1847/10/02 07:35
4	1871/10/13 03:30
5	1875/03/09 09:21
6	1900/01/20 06:33
7	1932/06/03 10:36
8	1932/06/18 10:12
9	**1934/11/30 02:05**
10	1941/04/15 19:09
11	1948/12/03 00:22
12	1973/01/30 21:01
13	1995/10/09 15:35
14	**2003/01/22 02:06**
15	2022/09/19 13:05

Bold earthquakes represent continental events induced by the 1932/06/03 and 1995/10/09 earthquakes, respectively.

canyon (Fig. 1)—the boundary between the Banderas fore-arc block to the northwest and the Jalisco fore-arc block (JFB) to the southeast. This also suggests that the areas north and south of the canyon are separate crustal blocks.

Seismicity Background and Data

Despite the high seismicity in the region, it was not until 1994 that seismicity studies with local networks began (Núñez-Cornú *et al.*, 2002). Subsequent instrumental deployments and works are described in Núñez-Cornú *et al.* (2018) and Marín-Mesa *et al.* (2019). The first stage of the Jalisco Seismic Accelerometric Telemetric Network (RESAJ) project began in 2010 as a part of the work developed by the academic group "Sismología y Volcanología de Occidente (SisVOc)" with the deployment of ten stations (Núñez-Cornú *et al.*, 2018). By 2018, 24 stations were operative in real time.

Using data from the Colima Telemetric Seismic Network (RESCO), Núñez-Cornú and Sánchez-Mora (1999) carried out a seismicity study in the area. These authors proposed a dip angle for the RP between 12° and 20° at the southeast edge of the JB. Núñez-Cornú *et al.* (2002) studied the seismicity along the Jalisco coast using data from RESCO and Red Sísmica de Jalisco (RESJAL), deployed ten digital seismograph stations to the west and north of JB in late 2001 by Civil Protection of Jalisco State and Universidad de Guadalajara, and analyzed 250 earthquakes distributed within three areas: Bahía de Banderas, Amatlán de Cañas–Ameca, and the coastal region related to the MAT. Using waveform analysis, Núñez-Cornú *et al.* (2002) characterized two types of earthquakes in this area: earthquakes generated within the slab (intraslab) and continental earthquakes hypocenters for which were in the slab–continent contact and continental crust. Moreover, they proposed that this slab dips at an angle of 15° up to 160 km from the trench and bends due to the oblique subduction. Other local seismicity studies agree with this (Núñez-Cornú *et al.*, 2002; Rutz-López and Núñez-Cornú, 2004).

The 22 January 2003 M_w 7.4 Armenia earthquake and associated aftershocks were studied by Núñez-Cornú *et al.* (2004) using data from the local networks (RESCO and RESJAL); the mainshock took place at 5.0 km depth. A study of aftershocks was carried out 72 hr after the main earthquake for the period 24–31 January using portable digital stations (Núñez-Cornú *et al.*, 2010). Based upon these observations and aftershock distribution, these authors proposed that the stresses generated by the oblique subduction in the contact with the continental crust caused the Armería earthquake. Based on this aftershock study, these authors also reported that the RP subducts at an angle of 12° from aftershock studies, as Núñez-Cornú and Sánchez-Mora (1999) proposed.

The geometry of the eastern part of the RP and the western part of the CP was studied by Gutiérrez-Peña *et al.* (2015) using seismicity recorded by the Mapping the Rivera subduction zone (MARS) experiment. Locating more than 2100 earthquakes, they proposed that the CP is slightly curved and dips at ~30°, whereas the RP presents a small dip angle in the coastal area increasing toward JB. However, hypocenters and the projected RP present no continuity in the profiles perpendicular to the trench. Parallelly to the trench and toward the CRZ, both the plates are subducting obliquely. It is possible to observe a dip angle that varies between 6° and 11° for the CP. Yang *et al.* (2009) process the MARS and Colima Deep Seismic Experiment (CODEX) databases to carry out a tomographic finite-frequency seismic study using 269 teleseismic earthquakes. Soto *et al.* (2009), using seismic anisotropy, propose a mantle model for the CP and RP. In another study using the MARS database and other two catalogs, Abbott and Brudzinski (2015) relocated nearly 1600 earthquakes (18 months) by applying an automated algorithm. They identified two areas with high seismicity: the first one in the epicentral region of the 2003 Armería earthquake and the region between the Tamazula fault and the Armería river (RR). These authors also reported seismicity in the 1995 earthquake epicentral area. Watkins *et al.* (2018) also process the MARS and CODEX databases using an automatic detection algorithm to locate 803 earthquakes used in a tomographic study.

Núñez-Cornú *et al.* (2016), using seismicity and wide-angle seismic data (WAS), found that the subducted plate thickness beneath Bahía de Banderas and Puerto Vallarta is at least 10 km with a subduction angle of 10°, whereas the depth of the continental crust beneath Puerto Vallarta is ~20 km.

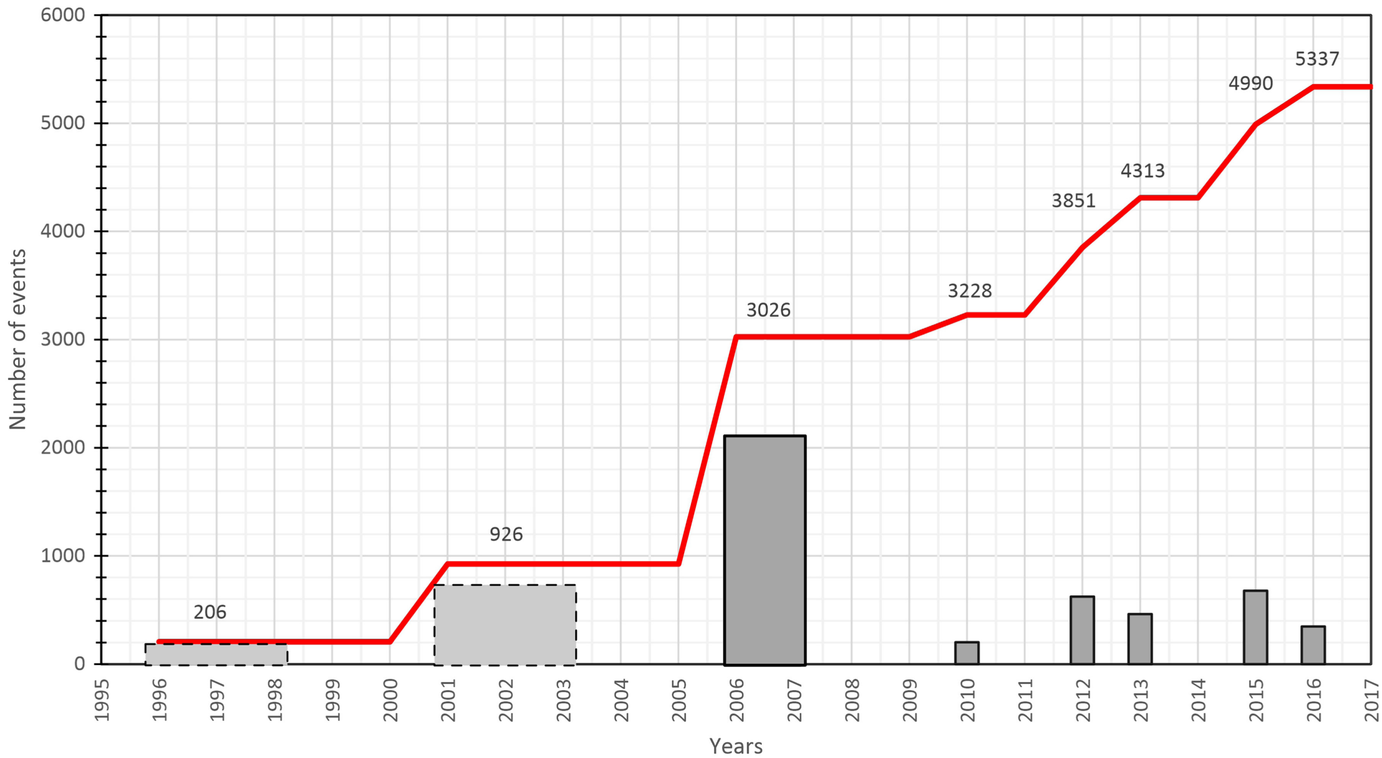

Figure 2. Number of events and periods of data registration used in this study. The red line denotes the cumulative number of events for our study. The dashed line blocks indicate noncontinuous period register data. The color version of this figure is available only in the electronic edition.

Carrillo-de la Cruz, *et al.* (2019) studied the Tres Marías basin (Fig. 1). Using marine multichannel seismic (MSC) data along a profile perpendicular to Sierra de Cleofas (SC), they found that RP is dipping with an angle of 6° and has a thickness of 7 km. From TsuJal project, Núñez *et al.* (2019) examined profile TS04 perpendicular to the coast using MSC and WAS data, and found a thickness of 7 km for the RP dipping 14°. The profile only extended to near the shoreline. Núñez-Cornú *et al.* (2021) study the oceanic and continental structure of the coast with a seismic profile (WAS and MSC) parallel to the coast from the Islas Marías Archipelago to Chamela village.

Marín-Mesa *et al.* (2019) studied the seismicity recorded by RESAJ from June to December 2015, locating 683 earthquakes with magnitudes between M_L 1.0 and 4.0. These authors suggest the existence of three seismogenic zones along the Jalisco coast: Bahía de Banderas, Purificación river (PR), and Minatitlán; and they identified two aseismic areas (ASA) *X* and *Y* (Fig. 2). The seismicity analysis perpendicular to the trench indicates that RP is dipping with an angle of 22° in the region of Bahía de Banderas, whereas a dip of 31° in the PR (Fig. 1) and 28° in Minatitlán (Fig. 1) is observed. Moreover, they analyzed the geometry of RP using profiles parallel to the trench; a dip of 26° to the southeast at 150 km from the trench and the ASA *Y* can be observed. A dip of 16° and ASA *X* and *Y* are determined at 100 km from the trench. Between the coastline and the trench, a dip angle of 12° in the southeast direction is suggested.

In this study, we use all the hypocenters available in the CA-SisVOc database, which includes the studies conducted from 1996 to 2015 (Núñez-Cornú and Sánchez-Mora, 1999; Nuñez-Cornú *et al.*, 2002, 2004, 2010; Rutz-López and Núñez-Cornú, 2004, 2013; Gutiérrez-Peña *et al.*, 2015; Marín-Mesa*et al.*, 2019), RESAJ relocated hypocenters for January–March 2016 were also included. We obtained a total of 5337 hypocenters located with the same methodology, Hypo71PC (Lee and Valdés, 1985) using the *P*-wave velocity model proposed by Núñez-Cornú *et al.*(2002). At least four *P* waves and two *S* waves readings were used, and we included only events with root mean square <0.50 s, error in horizontal (ERH) <10.0 km, and error in depth (ERZ) <10.0 km. Number of events and periods of data registration used in this study are shown in Figure 2.

Seismic Analysis

The objective of this work is to study the database of seismic hypocenters available for the JB and analyze the possibility of identifying structures associated with seismic patterns. A map of epicenters for all our events (Fig. 3) shows the main characteristics of the seismicity in the region, here we indicate the positions of the cross sections used to analyze the geometry of the slabs, which do not always agree with those cross sections studied by other authors.

From Figure 3 we observe that epicentral distribution is different over Michoacán block, CRZ, and JB. Distribution of seismicity on the Michoacán block starts almost at the

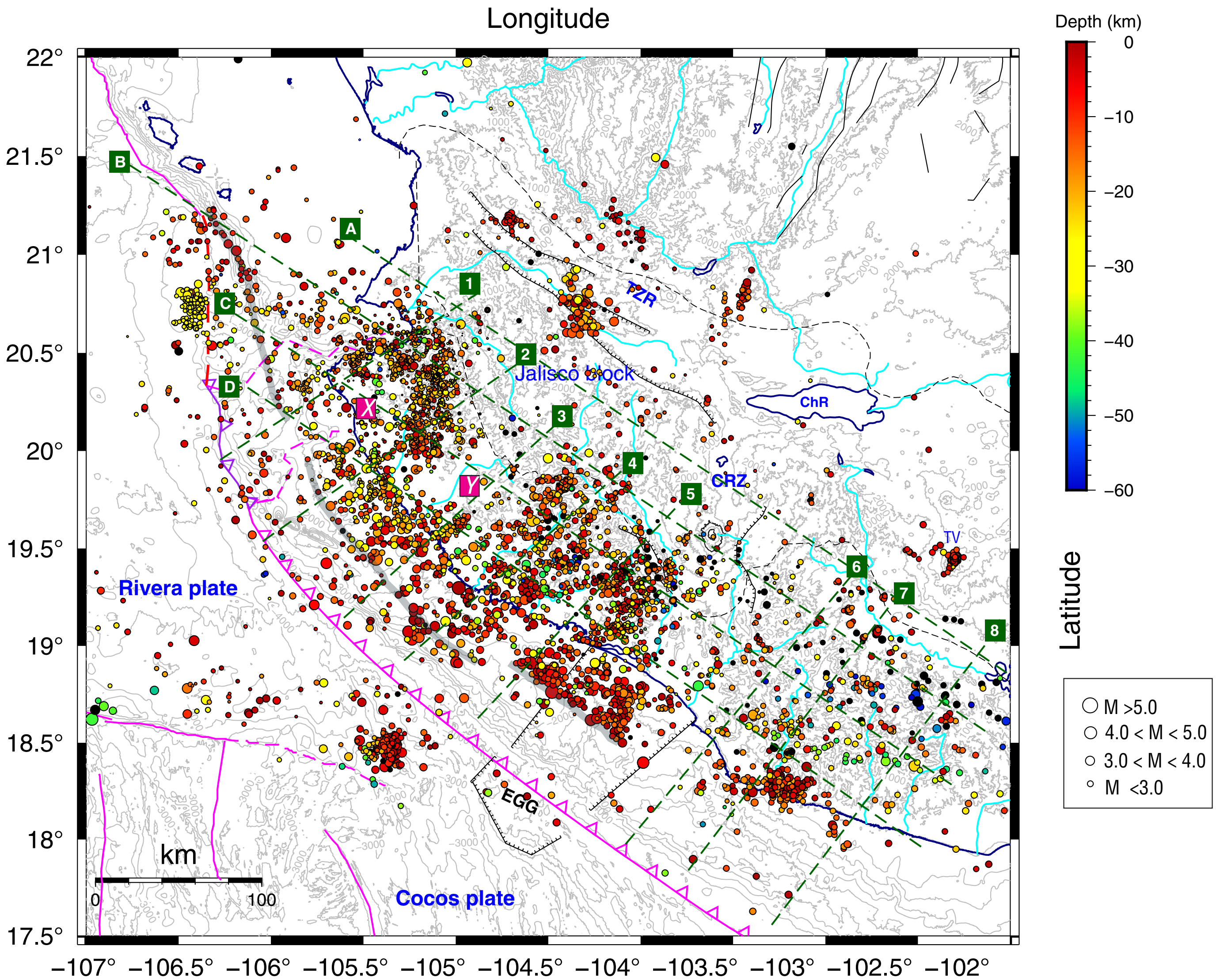

Figure 3. Epicentral map of the seismicity analyzed in this study. Profiles (in green squares): 1, 2, 3, 4, 5, 6, 7, 8, A, B, C, and D indicated. Abbreviations: ChR, Chapala rift zone; CRZ, Colima rift zone; EGG, El Gordo graben; TV, Tancítaro volcano; and TZR, Tepic-Zacoalco rift zone. Circle sizes scale by magnitudes, and color denotes event depth in kilometer. *X* and *Y* refer to aseismic zones proposed by Marín-Mesa *et al.* (2019). The gray lines depict the coupling zones between the slab and continental crust of Rivera plate (RP) and Jalisco block (JB). The color version of this figure is available only in the electronic edition.

coastline (~87 km from the trench) and looks roughly homogeneous, shallow near the coast, and deeper inland; a shallow seismic cluster is observed at the coast in the mouth of Coalcomán river (Fig. 1). Seismicity at CRZ is scarce, except near its borders and in the vicinity of Colima volcano. Within the JB we observe a heterogeneous epicentral distribution in agreement with some previous works: A frame of seismicity along the coast and offshore (at about 40 km from the trench) begins at SC (Fig. 1) and ends at the RR (Fig. 1), where the coupling zone between the slab and the continental crust generates a seismogenic zone due to the friction (CZ, gray line in Figs. 3 and 4), this seismic alignment continues parallel to the coast until CRZ and illuminates the seaward extent of seismogenic contact (CZ) between RP and NOAM. This feature can be divided into three segments: the first segment is from MCI (Fig. 1) to the area of the Ipala canyon (IC, Fig. 1), where scarce seismicity is observed. The second segment is south of the IC area to the Marabasco river (MR, Fig. 1), where an aseismic patch (perpendicular to the trench) of about 20 km wide is observed. Beyond this comparatively aseismic segment, the seismicity continues, but the CZ moves inland to ~60 km from the trench. Several seismic alignments and clusters are observed between Bahía de Banderas and the western limit of the CRZ (Fig. 1).

We observe that for the JB crustal and deeper seismicity stops northeastern of cross-section B (Fig. 3), except for the crustal seismicity of Bahía de Banderas seismogenic zone.

To study the seismicity characteristics, we split the region into three areas: north (Fig. 4a), center (Fig. 4b), and south (Fig. 3c), and plot cross sections along profiles perpendicular

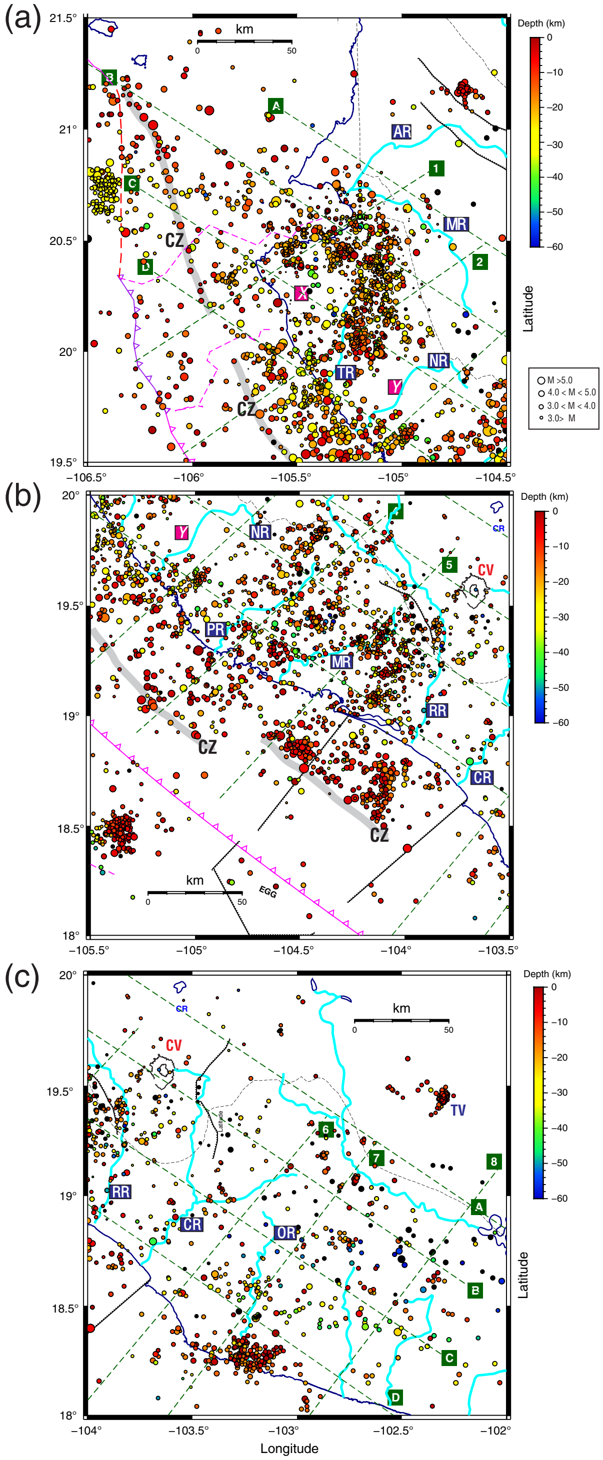

Figure 4. Seismicity map in: (a) northern Jalisco coast (Banderas fore-arc block); (b) southern Jalisco coast (JFB); and (c) Colima rift zone and west Michoacán areas. Circle sizes scale by magnitudes and color denotes event depth in kilometer. *X* and *Y* refer to aseismic zones proposed by Marín-Mesa *et al.* (2019). Letters in blue squares correspond to the rivers shown in Figure 1. Numbers and letters in green squares correspond to the profiles shown in Figure 2. The gray lines depict the coupling zones between the slab and continental crust of RP and JB. CV, Colima volcano; and TV, Tancitaro volcano. The color version of this figure is available only in the electronic edition.

(Fig. 5) and parallel to the trench (Fig. 6). Similar graphics for the CRZ are presented (Figs. 7 and 8).

Banderas fore-arc block

The seismicity in the northern area of the region or Banderas fore-arc block can be observed in Figure 4a. West of SC, a seismic cluster with a depth between 20 and 30 km is observed; this activity occurred as swarms (Tinoco-Villa, 2015). East of SC and south of MCI, a shallow seismic alignment defines the northern tip of RP and the beginning of subduction (Núñez-Cornú *et al.*, 2019). We observe seismicity distributed along the southern coast of Bahía de Banderas and west of the Tomatlán river (TR, Fig. 1) in a north–south direction. This horseshoe seismicity pattern delimits an area with sparse seismicity defined as ASA *X* by Marín-Mesa *et al.* (2019). To the southeast, the ASA *Y* is observed on both sides of the San Nicolás river (Fig. 1)—between the TR and PR (Fig. 1). Here, there is significant seismicity offshore between the coastline and the CZ. Figure 5a indicates a continental crust thickness of 25 km and a slab dipping at 24° up to 135 km from the trench to the cross-section A zone. Cross-section 2 (Fig. 5b) shows a crustal thickness of 25 km and a slab dipping 27° up to 95 km from the trench at the profile D area; Figure 5c also suggests a crustal thickness of 25 km, and a slab dipping 27° up to 90 km from the trench to the profile D area is also observed, ASA *Y* is observed beyond 95 km. In Figure 6a (red area) cross-section A, a dip angle of 18° is suggested for the slab in a southeasterly direction until a distance of about 145 km with a crustal thick of 25 km at cross-section 2 area. In cross-section B (red area in Fig. 6b), a dip of 13° is observed for the slab until 215 km in a southeasterly direction in the same region where the crust reaches 35 km thick; here, ASA *Y* is observed between 220 and 290 km. In cross-section C (red area in Fig. 6c), a dipping of 9° is observed in a southeast direction for the slab until 135 km at cross-section 2 area, where we observe a thickness for the crust of 25 km; here, the ASAs *X* and *Y* are observed. Profile D (red area in Fig. 6d) shows that the seismicity is offshore between the coastline and the trench, with the slab dipping 11° in a southeast direction until the Marabasco river (Fig. 1), where the seismicity suddenly stops. After profile 5 projection, the seismicity is observed again until CGW; in this region, the continental crust reaches a thickness of 35 km.

JFB

In Figure 4b within the JFB, in the central area, two crustal seismic alignments are visible at both sides of the PR, as well as seismicity along the Marabasco river, and between this river and the western zone of CRZ, defined as Purificación seismogenic zone (Marín-Mesa *et al.*, 2019). The seismicity ends at the western border of CRZ, marking the eastern border of RP. Seismic clusters offshore are related to the epicentral area for 9 October 1995 **M** 8.0 (west) and 22 January 2003 **M** 7.3 (east) earthquakes. Offshore seismicity near Paleo Rivera

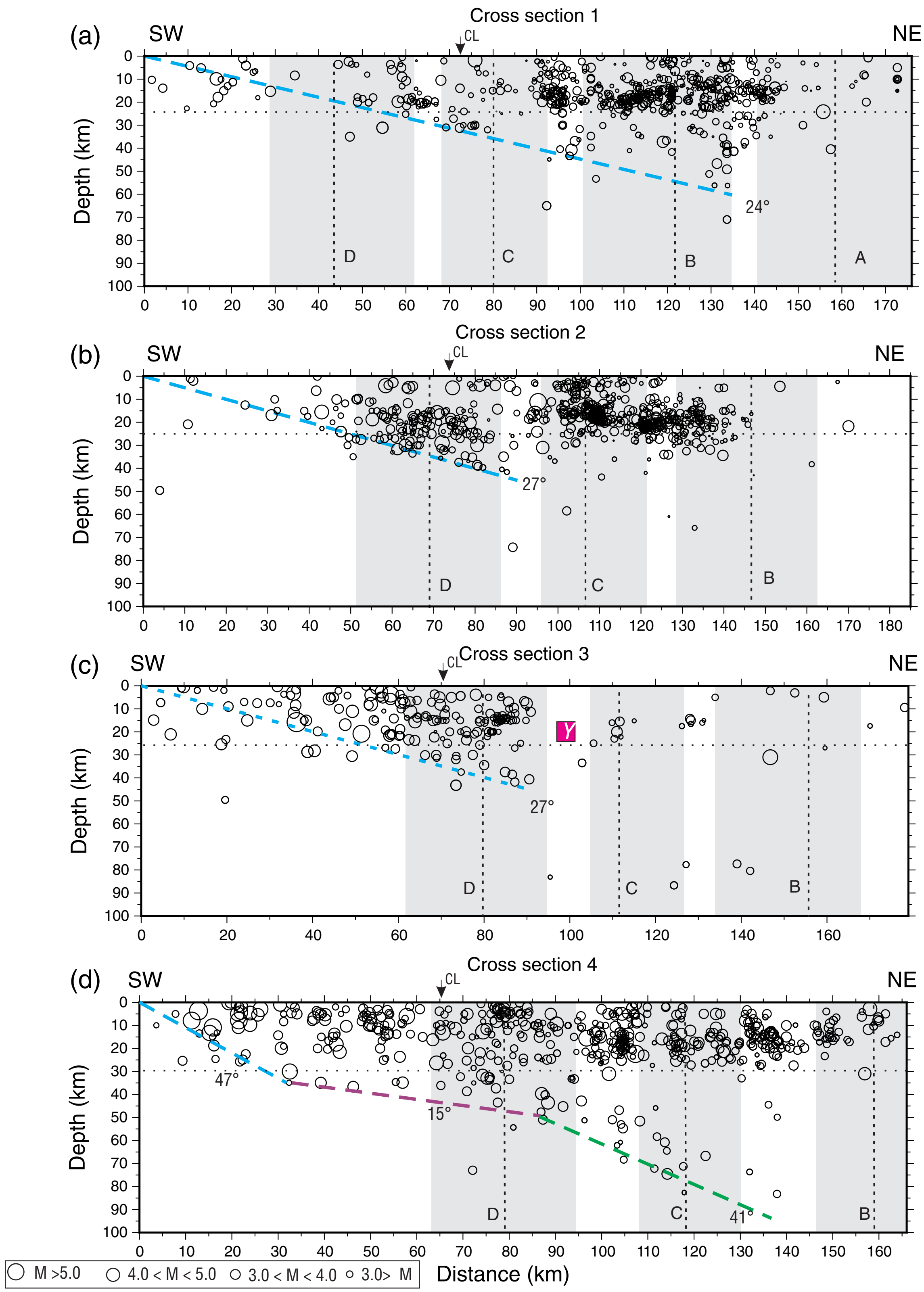

Figure 5. (a) Cross-section 1. Length 176 km; width 22 km west/22 km east. (b) Cross-section 2. Length 185 km; width 20 km west/20 km east. (c) Cross-section 3. Length 179 km; width 17 km west/17 km east. (d) Cross-section 4. Length 166 km; width 22 km west/22 km east. Circle sizes scale by magnitude. The blue, purple, orange, and green dashed lines denote the subducting slab. Abbreviations: CL, Coastline; CRW, Colima rift west border; and *Y* refers to aseismic zone proposed by Marín-Mesa *et al.* (2019). The gray area indicates bandwidth of profiles A, B, C, and D. (e) Cross-section 5. Length 175 km; width 15 km west/39 km east. (f) Cross-section 6. Length 203 km; width 28 km west/13 km east. (g) Cross-section 7. Length 200 km; width 9 km west/22 km east. (h) Cross-section 8. Length 218 km; width 22 km west/39 km east. The color version of this figure is available only in the electronic edition. (*Continued*)

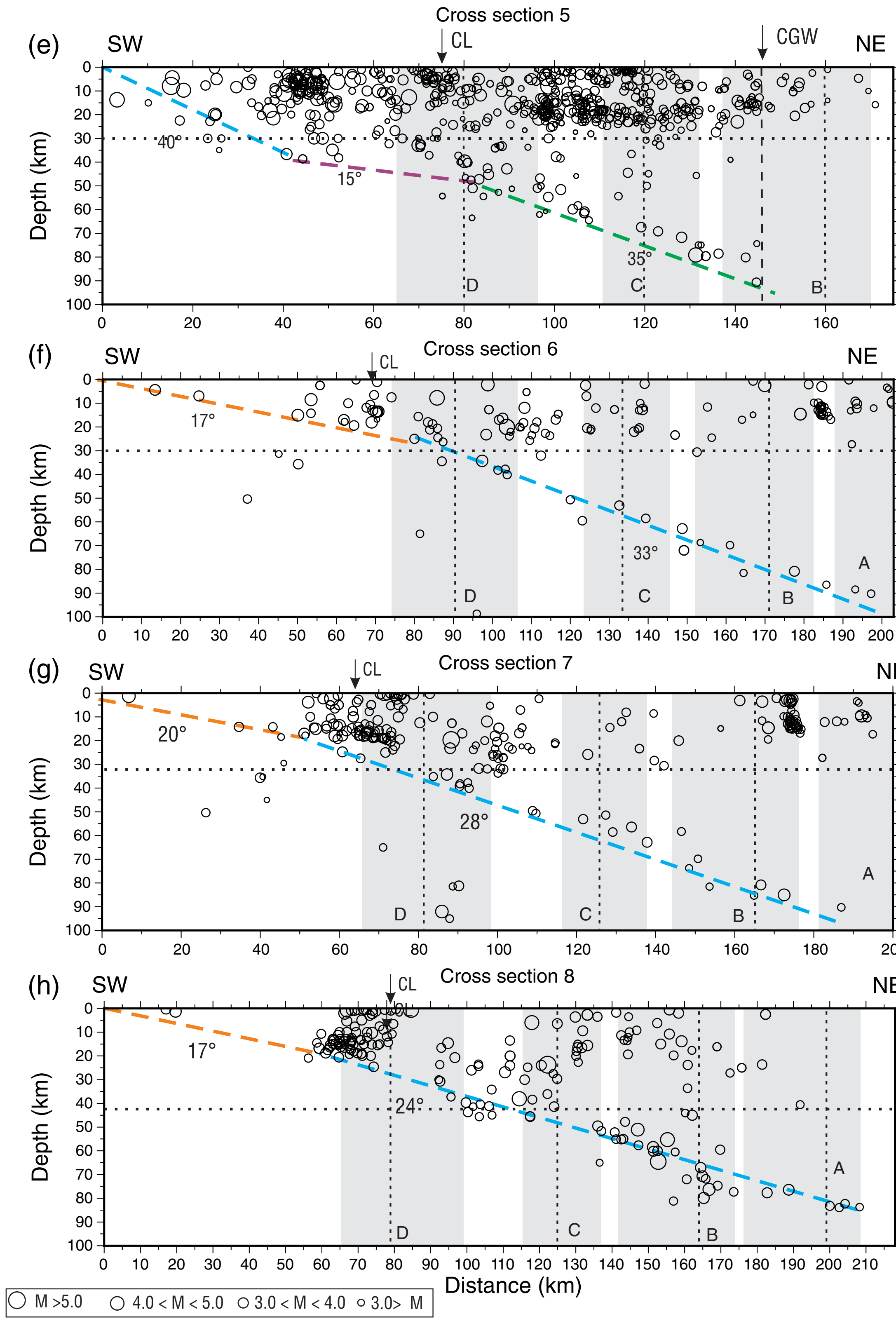

Figure 5. Continued

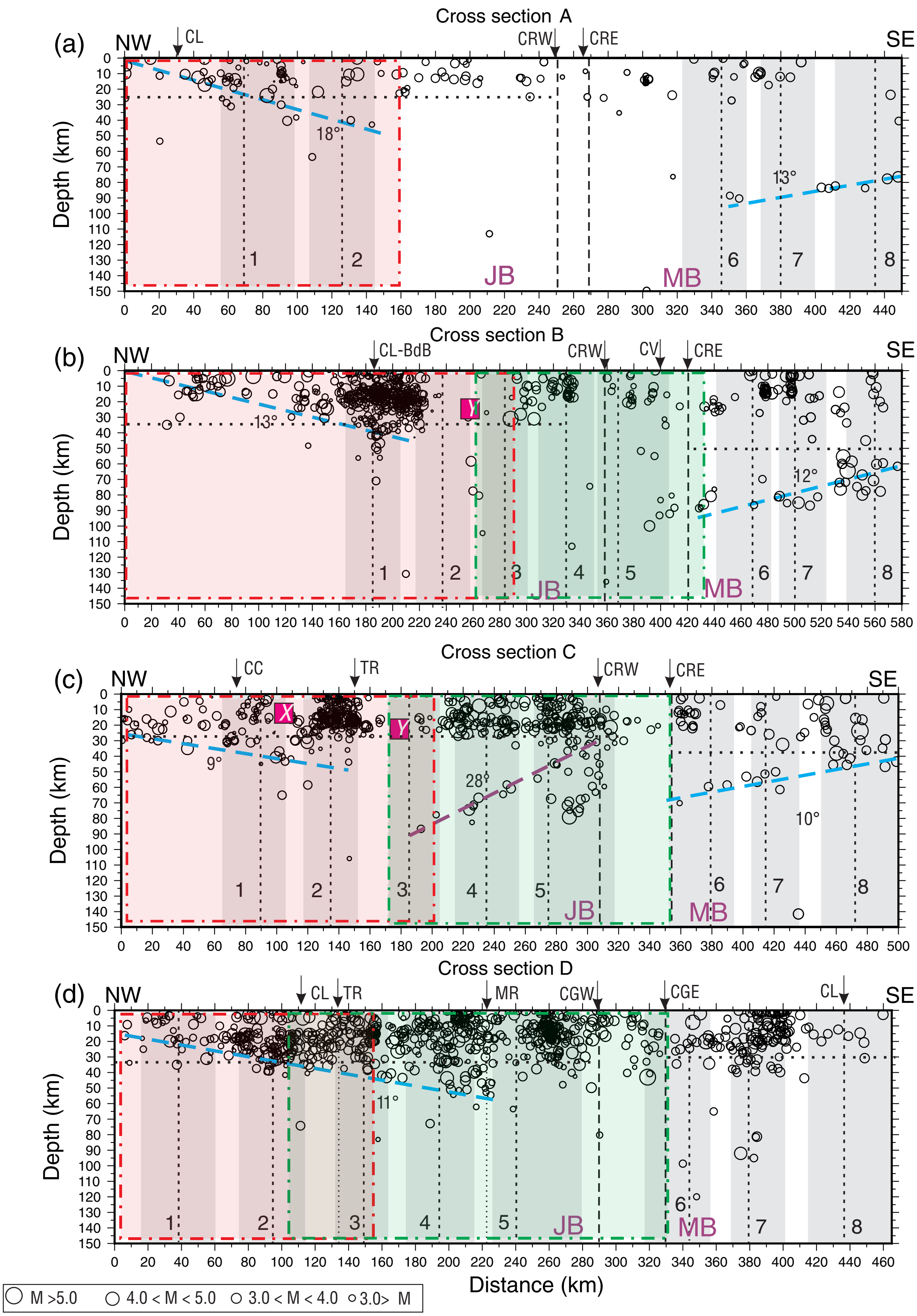

Figure 6. (a) Cross-section A. Length 445 km; width 17 km south/22 km north. (b) Cross-section B. Length 582 km; width 11 km south/22 km north. (c) Cross-section C. Length 501 km; width 11 km north/11 km south. (d) Cross-section D. Length 465 km; width 17 km north/17 km south. Abbreviations: CC, Cabo Corrientes; CL, coastline; CL-BdB, coastline–Bahía de Banderas; CRE, Colima rift east border; CRW, Colima rift west border; CV, Colima volcano; JB, Jalisco block; MB, Michoacán block; TR, TR; and *X* and *Y* refer to aseismic zones proposed by Marín-Mesa *et al.* (2019). The gray area indicates bandwidth of profiles 1, 2, 3, 4, 5, 6, 7, and 8. The red and green areas depict Banderas block and JFB, respectively. Circle sizes scale by magnitude. The blue and purple dashed lines denote the subducting slab. The color version of this figure is available only in the electronic edition.

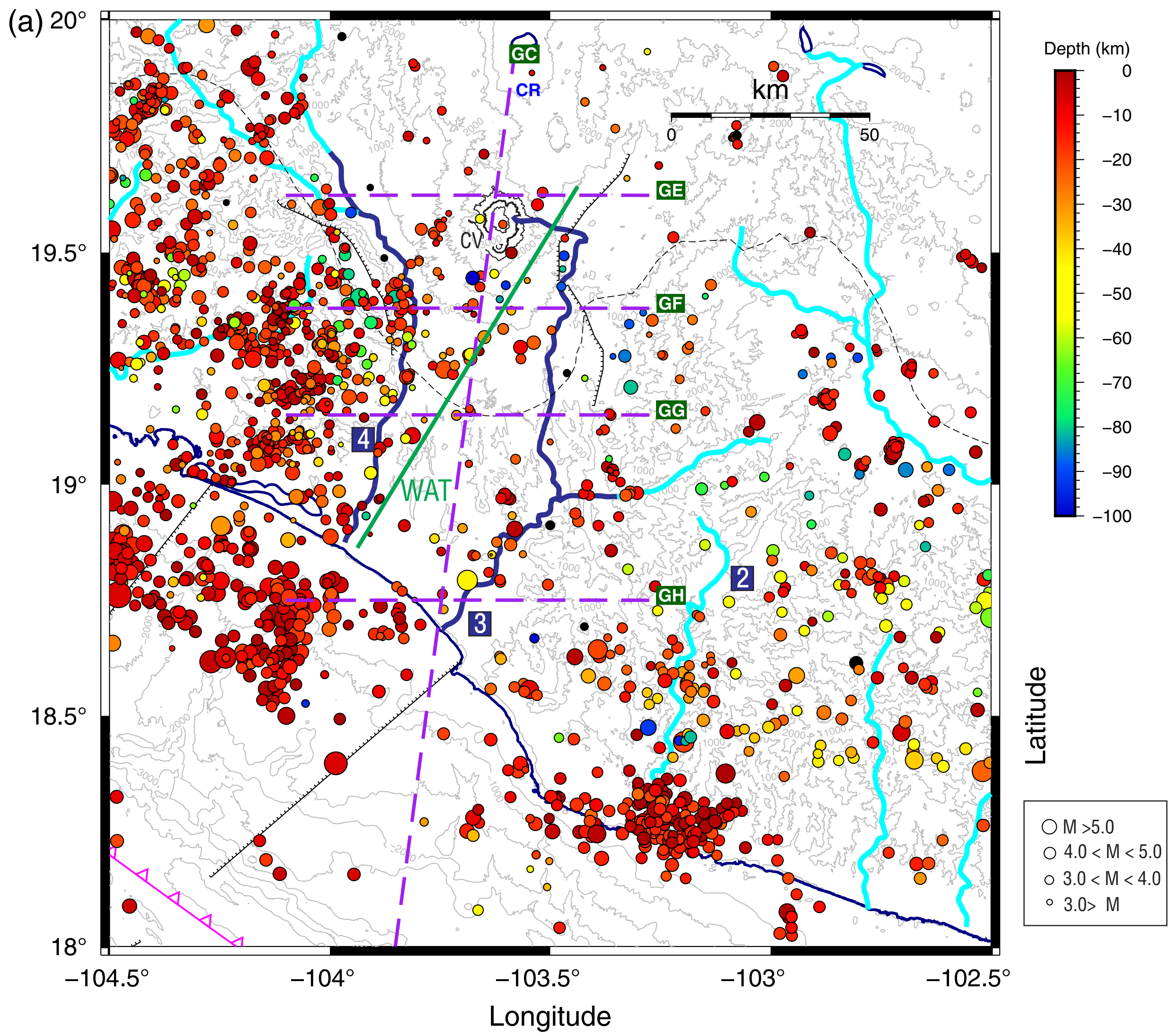

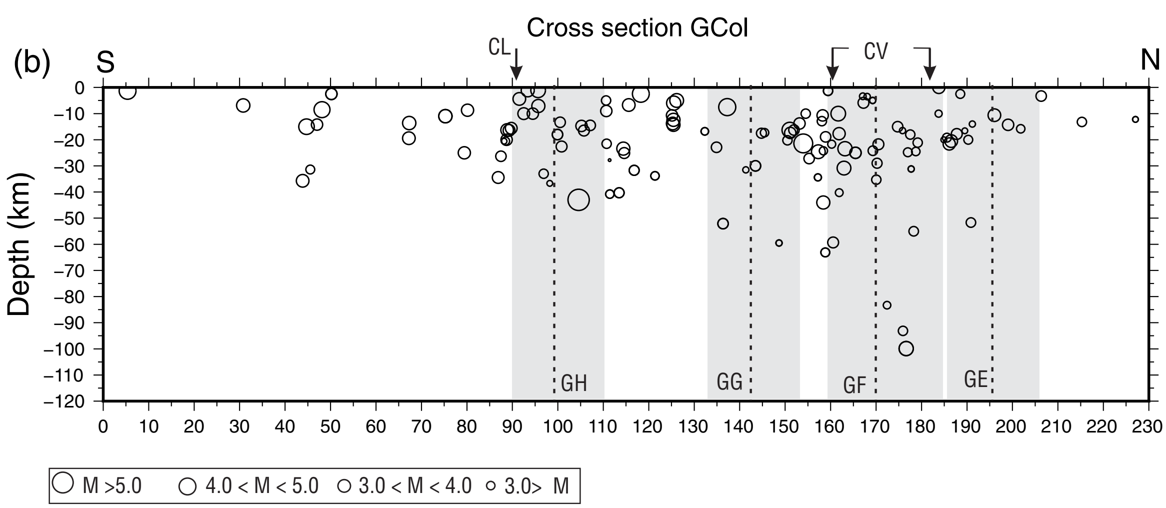

Figure 7. (a) Epicentral map of the Colima graben area. The green line depicts the wide-angle seismic transect (WAT) studied by Núñez Cornú *et al.* (1994). The purple dashed lines represent profiles shown in Figures 6b and 7. Numbers in blue squares shown rivers as Figure 1. Circle sizes scale by magnitudes, and color denotes event depth in kilometer. (b) Cross section along the Colima graben (GCol). Length 230 km; width 17 km east/22 km west. Abbreviations: CL, Coastline; and CV, Colima volcano. The color version of this figure is available only in the electronic edition.

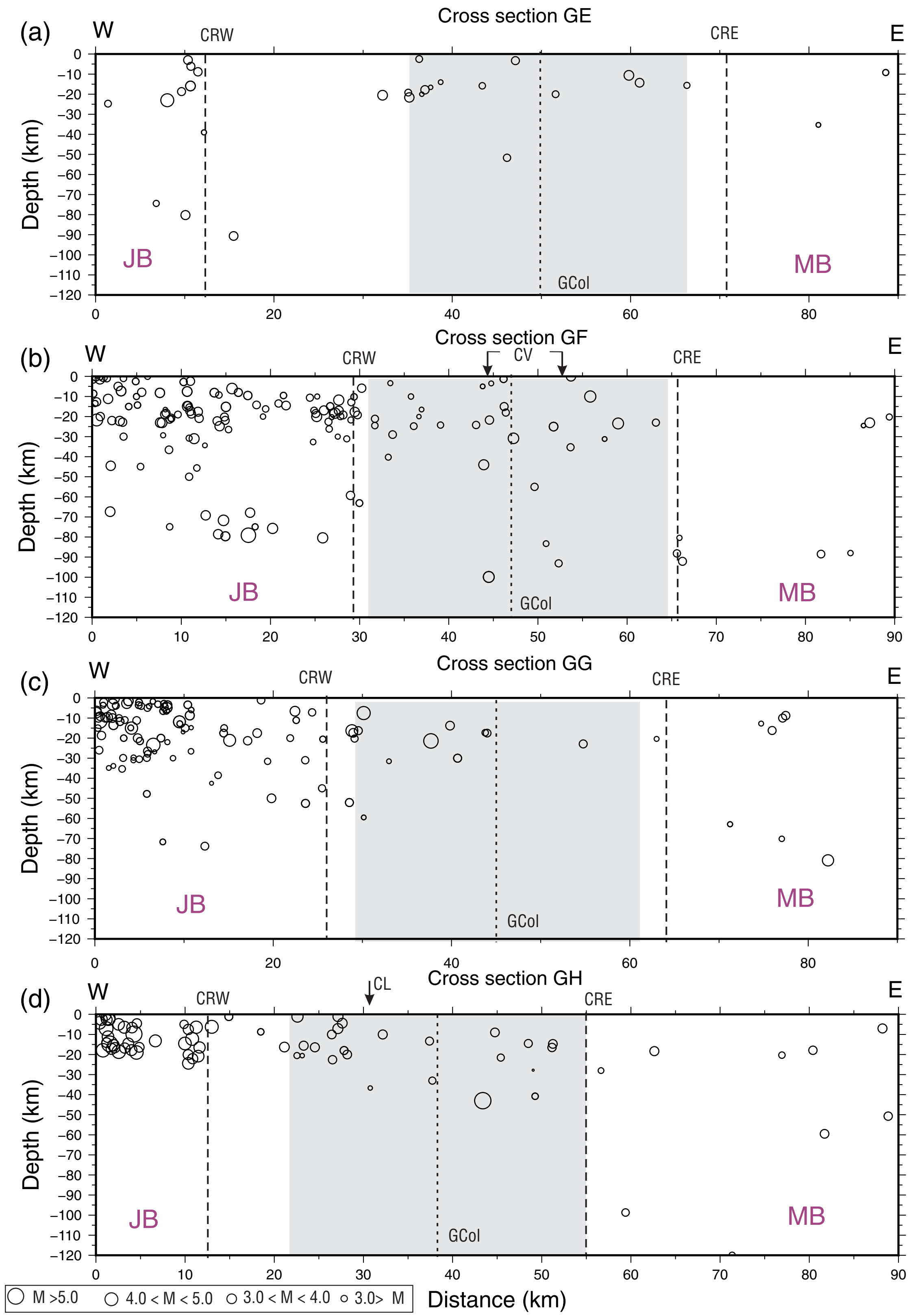

Figure 8. (a) Cross-section GE. Length 90 km; width 17 km south/22 km north. (b) Cross-section GF. Length 90 km; width 11 km south/22 km north. (c) Cross-section GG. Length 90 km; width 11 km north/11 km south. (d) Cross-section GH. Length 90 km; width 11 km north/11 km south. Abbreviations: CL, coastline; CRE, Colima rift east border; CRW, Colima rift west border; CV, Colima volcano; and JB, Jalisco block. The gray area corresponds to bandwidth of perpendicular profiles. The color version of this figure is available only in the electronic edition.

transform fault (Fig. 1) has been studied by Núñez-Cornú *et al.* (2021). In cross-section 4 (Fig. 5d), a fragmented slab is interpreted. From the trench to 30 km, a dip of 47° is inferred; from 30 to 90 km, we note a dip angle of 15°, and a dip of 41° is measured from 90 to 140 km; we observe a crustal thickness of 30 km. A similar pattern for the slab is observed in cross-section 5 (Fig. 5e), from the trench to 25 km, a dip of 40°, from 25 to 80 km, a dip of 15°, and from 80 to 145 km dipping to 35°; crustal thickness observed is also of 30 km. In cross-section B (Fig. 6b), seismicity between profiles 3 and 4 suggests a crust that is 35 km thick. In cross-section C (Fig. 6c) at the green area, the crustal and slab seismicity stops at the western border (CRW) of CRZ. A seismic alignment, 130 km long westward, starting at CRW, at 30 km depth until profile 3 at 85 km depth, with a dip of 28° in a northwest direction, can be seen; it crosses the areas of cross-sections 3, 4, and 5. The seismicity between 50 and 80 km depth around cross-section 5 corresponds to the limit of the edge of the slab. In cross-section D (green area in Fig. 6d), where the seismicity is offshore between the coastline and the trench, we observe that the slab tilts 11° in a southeast direction to the Marabasco river (Fig. 1), where the seismicity stops suddenly. After the projection of profile 5, the seismicity is observed again up to CGW. In this region, the continental crust reaches a thickness of 35 km.

Michoacán block

For the western Michoacán block, seismicity is plotted in Figure 3c. Here, we observe that, unlike the RP, the seismicity between the coast and the trench is sparse. A seismic cluster at the mouth of Cohuayana river (CR, Fig. 1) agrees with the epicentral area of the 1973 and 2022 earthquakes (Fig. 1), while the remaining seismicity is evenly distributed. A seismic cluster is observed in the northeast area of the region at the Tancítaro volcano zone, and this activity was studied by Pinzón *et al.* (2016). In cross-section 6 (Fig. 5f), we inferred two sections for the slab: the first from the trench inland 80 km with a dip of 17°, the second from this 80 km position to 200 km with a dip of 33°; we estimate a crustal thickness of 30 km. In Figure 5g, cross-section 7, the slab is also manifested in two segments: the first one from the trench inward 50 km with a dip of 17°, and the second from 50 to 190 km inland with a dip of 28°; a 32 km thick crust is observed for the continental crust. Cross-section 8 (Fig. 5h) exhibits two segments again: one from the trench to 65 km with a dip of 17°, and the second from 65 to 210 km with a dip of 24° with a crustal thickness of 40 km and sparse seismicity. The Cocos slab with a length of 100 km is observed in profile A (Fig. 6a) between profile 8 at 75 km depth and profile 6 at 95 km depth, dips 13° westward; there is insufficient data to estimate the continental crust thickness. In cross-section B (Fig. 6b), we observe the Cocos slab between profiles 8, at 60 km depth, and CRE, at 100 km depth, with a length of 160 km dipping 12° westward; a 50 km crustal thickness is inferred. Figure 6c (cross-section C) shows the Cocos slab from profile 8 to CRE with a length of 140 km dipping in a northwest direction, 10° between 40 and 70 km depth; a continental crust of 35 km thick can be inferred. In cross-section D (Fig. 6d), we do not observe the slab clearly; a continental crust of 30 km is observed; the seismic cluster associated with 2022 and 1973 earthquakes near profile 7 can be seen.

CRZ

The seismicity at CRZ is shown in Figures 7 and 8; the CRZ is between CR and RR (Fig. 1) and is oriented roughly north–south. Seismicity within the CRZ is sparse, although there is some seismicity offshore and near Colima volcano (Fig. 1). Along cross-section GCol (Fig. 7b), we infer a crustal thickness of 35–45 km, more profound events are observed below Colima volcano in the GF cross-section area; these may be associated with the volcano magmatic plumbing system. We do not observe any seismic evidence of a slab under CRZ, in contrast to cross-sections 5 and 6. The seismicity in the GE profile (Fig. 8a) is sparse and resides between 0 and 30 km depth at the GCol profile area. In Figure 8b, the seismicity in the GCol cross-section area occurs between 0 and 40 km; deeper seismicity is observed under Colima volcano, which, again, may be associated with the volcano. In Figure 8c, seismicity is sparse in the GCol profile area. Figure 8d shows the seismicity on the western side of GCol profiles concentrated offshore. Meanwhile, the seismicity on the eastern side may be associated with the edge of the Cocos plate.

Discussion

We use the most comprehensive local seismicity database available to analyze the regional seismically active features that define the geometry of tectonic structures in the western region of Mexico. This analysis shows that seismic patterns associated with the subduction process of the RP and Cocos plate below the North American plate are different.

Shallow seismicity (depth <30 km) in the JB (Fig. 9a) presents different seismic patterns and clusters; meanwhile, at the Michoacán block, the seismic activity is "random" distributed, except for the seismic cluster near the region where the 1973 and 2022 earthquakes occurred. The CRZ marks a clear separation between both the continental blocks. The Colima volcano edifice looks to have emerged between both the blocks and may act like a pull-apart mechanism to the blocks. The RR defines the western border of the JB.

At the Colima rift, we record insufficient seismicity to clearly define the thickness of the crust (Figs. 7b and 8). Núñez Cornú *et al.* (1994) conducted a refraction experiment to study the crust at the CRZ, their longest profile perpendicular to the trench (green line, Fig. 7) was Zapotiltic–El Real (110 km), and they did not report the Moho depth. Based on refraction penetration depth as a function of offset, this implies that the thick crust should be greater than 35 km.

The seismic patterns at JB suggest the existence of several structures (Fig. 9b). It is clear that the Jalisco subduction zone

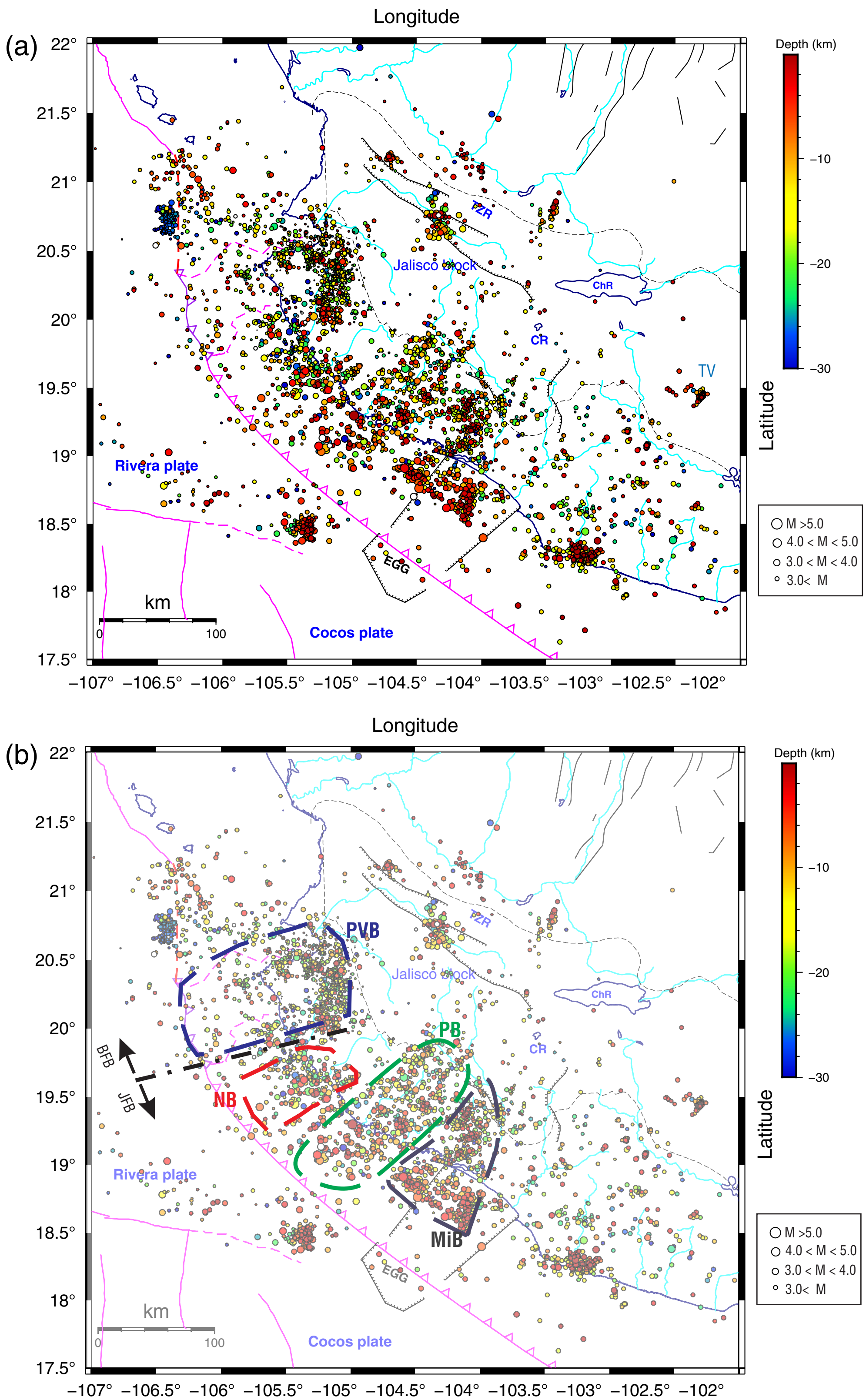

Figure 9. (a) Seismicity map with depth <30 km. (b) Crustal blocks proposed from north to south: MiB, Minatitlán block; NB, Nicolás block; PB, Purificación block; PVB, Puerto Vallarta block. Abbreviations: BF, Bandy fault; BFB, Banderas fore-arc block; ChR, Chapala rift zone; CRZ, Colima rift zone; EGG, El Gordo graben; JFB, Jalisco fore-arc block; and TZR, Tepic-Zacoalco rift zone. Circle sizes scale by magnitudes, and color denotes event depth in kilometer. The color version of this figure is available only in the electronic edition.

is segmented. The Banderas block and JFB are separated by the Bandy fault near the IC and TR. At the Banderas fore-arc block, we observe an area defined by a horseshoe-shaped seismic pattern along the TR and south of Bahía de Banderas; this surrounds ASA *X*, which can be considered a crustal block. This block can be associated with the Puerto Vallarta batholite (Gutiérrez Aguilar, 2019), and we have termed it the Puerto Vallarta block (PVB, Fig. 9).

At the JFB, we observe at least three crustal blocks. East of Bandy fault, we observe the San Nicolás block (Fig. 9b). The seismicity starts at CZ and stops abruptly at about 90 km eastward from the trench (20 km from the coastline). Beyond this, the ASA *Y* continues landward. The structure of the slab and the crust in this area was studied by Núñez-Cornú *et al.* (2019) using the wide-angle seismic profile TS04 from the TsuJal project, which is very near to profile 3 (Fig. 5c). There is no clear surface feature to identify the east border of this block in the Chamela area (Fig. 1). The next block to the southeast is the Purificacion block (PB, Fig. 9b), characterized by seismic alignments parallel to PR, as observed in cross-section 4 (Fig. 5d). Here, crustal seismicity occurs up to 170 km from the trench, and its crustal thickness is about 30 km. The eastern limit of the PB is defined by an aseismic patch of ~20 km wide, perpendicular to the trench, that begins at the mouth of the Marabasco river. East of this strip is the Minatitlán block (MiB, Fig. 9b) in which we observe that the CZ is offset

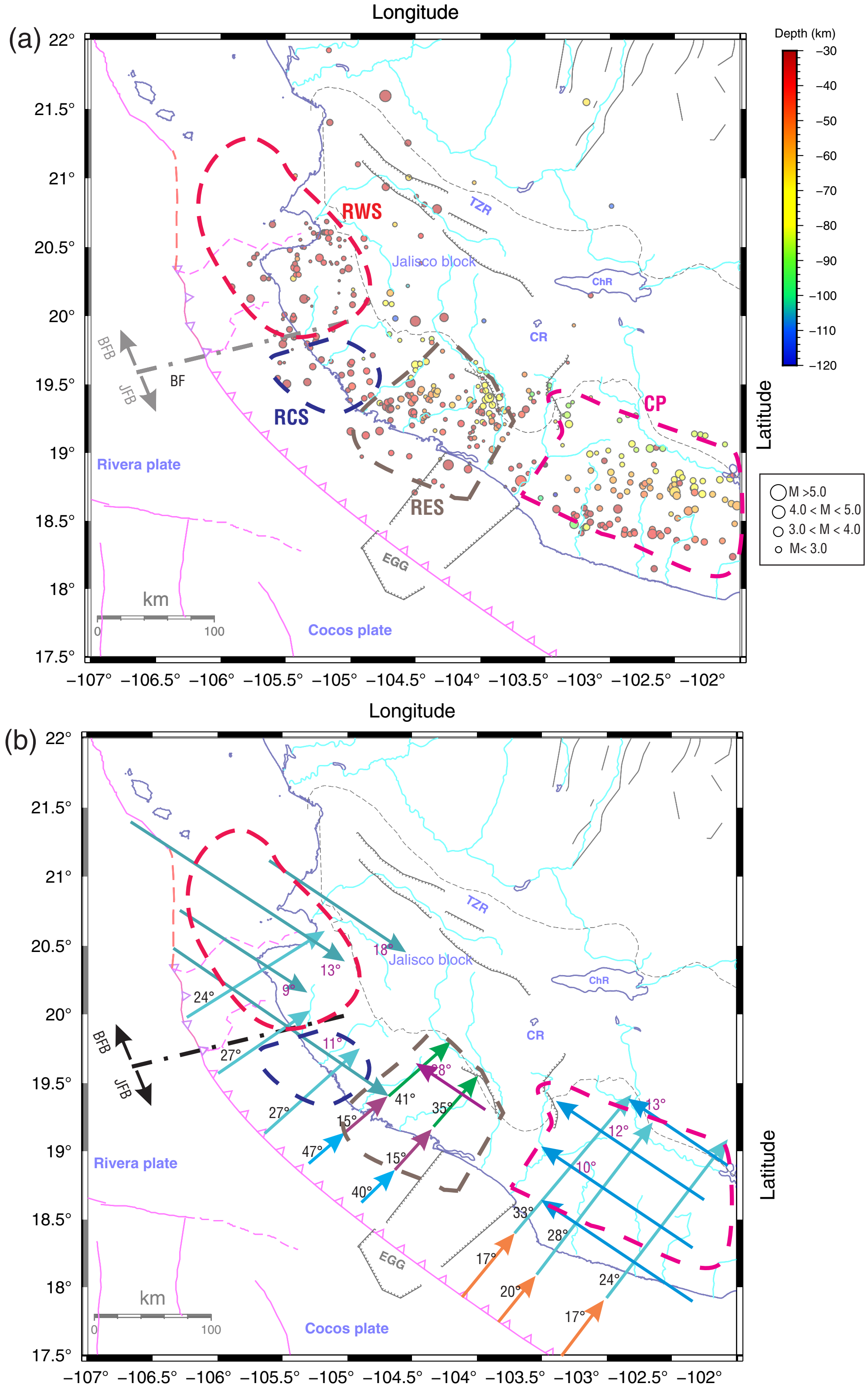

Figure 10. (a) Seismicity map with depth >30 km. Closed dashed lines represent the area of each segment of the RP proposed in this work. (b) Tilt vector (arrow) map. Dip angles represented next to every arrow. Abbreviations: BF, Bandy fault; BFB, Banderas fore-arc block; ChR, Chapala rift zone; CP, Cocos plate; CR, Colima rift; EGG, El Gordo graben; JFB, Jalisco fore-arc block; RCS, Rivera plate central segment; RES, Rivera plate east segment; RWS, Rivera plate west segment; and TZR, Tepic-Zacoalco rift zone. The color version of this figure is available only in the electronic edition.

by 20 km inland; the eastern border of MiB is the RR. Between the trench and the coast, we observe the 1995 (west) and 2003 (east) earthquake epicentral areas. Inland, seismicity is located between the northern segment of the Marabasco river and RR (Fig. 4a,b).

In Figure 10a, we show all hypocenters with a depth greater than 30 km. Based on this seismicity, clear differences can be seen between the RP and the CP separated by the CRZ. The CP is a single structure, whereas for the RP we identified three structures: one to the north of the Bandy fault, the Rivera western segment (RWS) in the Banderas fore-arc block, and two in the JFB, the Rivera central segment (RCS) and the Rivera eastern segment (RES; Fig. 10).

Figure 10b shows the tilt vectors obtained from profiles in Figures 5 and 6, superimposed on structures to illuminate the geometry of these structures. The subduction process of the CP is most closely approximating a typical process with a dip angle that ranges from east to west from 24° to 33°. The slab presents a bend in the northwest direction and increases in depth up to 13°. This bend suggests that the seismic radiation patterns are oriented in a northwest direction—the reason why the large earthquakes that occur in Michoacán cause so much damage in the eastern region of Jalisco and agrees with the rupture directivity observed by Singh *et al.* (2023). The RP is segmented into three units: one the RWS in the BFB and two segments the RCS and the RES in the JFB. The three segments display different geometries and sizes. The larger segment is the RWS; its geometry is similar to the geometry expected for the RP due to the process of oblique subduction dipping with an angle between 24° and 27° and bending slightly (13°) in a southeast direction, as previously published by Urías-Espinosa *et al.* (2016). To the south of the Bandy fault is the RCS, which is the smallest segment. This presents features similar to the RWS in the dip angle, perpendicular to the trench, and bending along the coast (Fig. 6d). A small gap in the seismicity corresponding to the Bandy fault is observed at 160 km. Landward the seismicity ends at 90 km from the trench (Fig. 5c); in contrast to ASA *Y*, it seems that this segment is truncated. From Figure 4d,e, we interpret the RES as a fragmented slab with a dip of 41° and a depth of 90 km at 140 km from the trench. Nevertheless, Figure 6c shows that the slab, with a width of 130 km, has an inclination of 28° to the northwest, perpendicular to the subduction direction. We suggest that after the separation of the Banderas block and JFB, the complex stress pattern in the JFB caused segmentation of the slab and fracture or truncation of the RCS. The truncated segment dragged down the RES, explaining also the inland shift of the CZ (Fig. 4c). We do not, however, observe clear evidence of the subducted truncated slab.

Different models based on seismic data have been proposed to define the RP and CP geometry; most assume a regular geometry for both the plates. The most recent studies use the MARS database, also included in our study. However, the coverage of the MARS network on the northern coast of Jalisco is very poor. Seismicity studies using MARS and CODEX data (e.g., Yang *et al.*, 2009; Watkins *et al.*, 2018; Abbot and Brudzinski, 2015) differ slightly from the results obtained by our group. We differ in how we process and analyze the data; we carefully choose the places to draw the profiles and define the bandwidth of the profiles used to identify possible structures.

Yang *et al.* (2009) state that beneath the northern part of the CRZ at a depth of 150 km, there is a gap between the RP and the Cocos plate, and they behave as two independent subduction processes from this point on. In this model, the RP and CP, after 100 km depth, increase their subduction angle to more than 60°, reaching more than 200 km depth under the Mexican volcanic axis. Other authors have used this model (e.g., Soto *et al.*, 2009; Manea *et al.*, 2013) as a basis for their studies.

Our seismicity study shows that the two plates are separated from the trench by the CRZ (under which no slab was identified), and that each plate has its geometry and different rheological characteristics. On both the plates, the deepest earthquakes we located are at 100 km; so we do not have information below this depth. The difference is that the method used by Yang *et al.* (2009) does not have enough resolution to see small structures in the upper crust. The bandwidth used by Watkins *et al.* (2018) and Abbot and Brudzinski (2015) in their profiles needs to be narrower to identify the crustal structures.

Until now, the existence of a segmentation in the RP had not been proposed; the previous hypothesis assumed a simple geometry for the RP that broke in its entirety with the two earthquakes of 1932 (Singh *et al.*, 1985) but not explains the 1934 earthquake (earthquake 9, Fig. 1) with epicenter in the PVB; however, there is no relevant data about a tsunami generated by this earthquake (Trejo-Gómez *et al.*, 2021), it was probably a crustal earthquake like the one in 2003 (earthquake 14, Fig. 1; Núñez-Cornú *et al.*, 2004, 2010). These earthquakes (1934 and 2003) took place a short period after the big earthquakes (1932 and 1995), which suggests that they were induced by the stress liberated by the big earthquakes. The seismic hazard in the region should be reevaluated due to the possibility of earthquakes $\mathbf{M} > 7.0$ in the crustal blocks.

Trejo-Gómez *et al.* (2021) modeled the run-up and the extent of flooding generated by the tsunami caused by the 1995 earthquake. For this, they used a simplified seismic source model corresponding to an earthquake M_w 8.0 with a rupture area of $A = 9000$ km^2 ($L = 150$ km, $W = 60$ km) with a heterogeneous coseismic dislocation divided into two sectors: the eastern sector, between the CRW and Careyes (Fig. 1) with a length of 90 km and a width of 60 km and dislocation of 3 m, and the western sector west of Careyes with a length of 60 km and a width of 60 km with a displacement of 1 m. A rough correlation is observed between the eastern sector with the RES and the western sector with the RCS. Under this hypothesis, the 1995 earthquake would have been generated by the slip of the RES and RCS sectors, and the slip of RWS and RCS caused the 1932 June 3 earthquake while the 18 June 1932 by the slip of RES.

The strength of the interpretation presented in this work lies in the fact that, although we do not have a continuous catalog of earthquakes, the reported seismicity allows us to clarify the existence and geometry of multiple tectonic structures, some of which may give rise to large magnitude events.

Conclusions

The main conclusions of this study are:

1. The data analyzed supports the fracture of the Jalisco subduction zone into at least two fore-arc blocks, the Banderas block and JFB, separated by the Bandy fault.
2. The crustal thickness of the JB in this region is ~30 km.
3. Shallow seismicity on the Jalisco coast suggests the existence of four blocks.
4. Deep seismicity indicates that the RP is divided into three segments: the Rivera west segment, the RCS, and the RES.
5. The RWS from SC to the Bandy fault subducts at an angle of 24° up to 135 km from the trench, reaching a depth of 55 km. This is slightly bent in a southeasterly direction.
6. The RCS between the Bandy fault and PR subducts at an angle of 27° and reaches a depth of 45 km at 90 km from the trench; it seems truncated.
7. The RES presents staggered subduction angles and is bent northwesterly, reaching a depth of 90 km at 145 km from the trench.

8. No seismic evidence of a slab under the CRZ was found. The crustal thickness is greater than 35 km.
9. The crustal thickness of the Michoacán block in this region is ~35 km.
10. Cocos plate subducts with an angle that varies between 24° and 33° perpendicular to the trench and is bent 12° to the northwest, reaching a depth of 100 km at 210 km from the trench.

These results suggest that the current seismotectonic models of the region should be revised.

Data and Resources

All geophysical data collected by Jalisco Seismic Accelerometric Telemetric Network (RESAJ) are in a database at CA-UDG-276 Sismología y Volcanología de Occidente (SisVOc). The data may be available for use in collaborative research projects between CA-SisVOc and other interested institutions by specific agreements. For more information, please contact pacornu77@gmail.com. The authors used the Generic Mapping Tools (GMT) version 6.2 (Wessel *et al.*, 2019) to generate maps and profiles.

Declaration of Competing Interests

The authors acknowledge that there are no conflicts of interest recorded.

Acknowledgments

The authors acknowledge Charlotte Rowe for her comments, observations, and English revision, which significantly improved the article. The authors are very grateful to the reviewers, because their thorough and thoughtful comments improved our article significantly. The authors thank C. Quinteros for allowing us to use her Generic Mapping Tools (GMT) codes. Different projects funded this research: CONACyT-FOMIXJal 2008-96567 (2009), 2008-96539 (2009), 2010-149245 (2010), COECyTJAL 0406-104692023, and UdeG internal Projects. Author Contributions: F. J. N. C. supported conceptualization, methodology, investigation, data processing, data analysis, conclusions, funding acquisition, and original draft writing. C. S. P. supported data analysis, edition, and funding. D. N. supported conceptualization, methodology, investigation, review, and editing.

References

Abbott, E. R., and M. R. Brudzinski (2015). Shallow seismicity patterns in the northwestern section of the Mexico subduction zone, *J. South Am. Earth Sci.* **63,** 279–292, doi: 10.1016/j.jsames.2015.07.012.

Beck, M. E., Jr. (1991). Coastwise transport reconsidered: lateral displacements in oblique subduction zones, and tectonic consequences, *Phys. Earth Planet. In.* **68,** 1–8.

Carrillo-de la Cruz, J. L., D. Núñez, F. J. de Escalona-Alcázar, F. J. Núñez-Cornú, A. González-Fernández, D. Córdoba, and J. J. Dañobeitia (2019). Tectonic analysis of the southern of María Cleofas island from bathymetric and seismic data, *Seismol. Res. Lett.* **90,** no. 5, 1748–670, doi: 10.17885/0220180398.

Dañobeitia, J. J., R. Bartolomé, M. Prada, F. J. Nuñez-Cornú, D. Córdoba, W. L. Bandy, F. Estrada, A. L. Cameselle, D. Nuñez, and A. Castellón (2016). Crustal architecture at the collision zone between Rivera and North American plates at the Jalisco block: Tsujal project, *Pure Appl. Geophys.* **173,** 3553–3573, doi: 10.1007/s00024-016-1388-7.

DeMets, C., and S. Stein (1990). Present-day kinematics of the Rivera plate and implications for tectonics in southwestern México, *J. Geophys. Res.* **95,** 21,931–21,948.

Escobedo, D., J. Pacheco, and G. Suarez (1998). Teleseismic body-wave analysis of the 9 October 1995 (M_w 8), Colima-Jalisco, Mexico earthquake, and its largest foreshock and aftershock, *Geophys. Res. Lett.* **25,** 547–550.

Fitch, T. J. (1972). Plate convergence, transcurrent faults, and internal deformation adjacent to southeast Asia and the western Pacific, *J. Geophys. Res.* **77,** 4432–4460.

Frey, M., R. A. Lange, C. M. Hall, H. Delgado-Granados, and S. E. Carmichael (2007). Al Pliocene ignimbrite flare-up along the Tepic-Zacoalco rift: Evidence for the initial stages of rifting between the Jalisco block (Mexico) and North America, *Geol. Soc. Am. Bull.* **119,** nos. 1/2, 49–64.

Gutiérrez-Peña, Q. J., C. R. Escudero, and F. J. Núñez-Cornú (2015). Geometry of the Rivera–Cocos subduction zone inferred from local seismicity, *Bull. Seismol. Soc. Am.* **105,** 6, 3104–3113.

Gutiérrez Aguilar, F. (2019). Geocronología, isotopía Sr-Nd y modelado de fases en equilibrio: Avances en la petrogénesis del Complejo Metamórfico Chimo-Yelapa en el estado de Jalisco, México, *Master Thesis*, Posgrado en Ciencias de la Tierra, UNAM, 187 pp.

Jarrard, R. D. (1986). Terrain motion by strike-slip faulting of forearc slivers, *Geology* **14,** 780–783.

Kostoglodov, V., and W. Bandy (1995). Seismotectonic constraints on the convergence rate between the Rivera and North American plates, *J. Geophys. Res.* **100,** no. B9, 17,977–17,989.

Lee, W. H. K., and C. M. Valdés (1985). A personal computer version of the hypo71 earthquake location program, *U.S. Geol. Surv. Open-File Rept. 85-749*.

Luhr, J., S. Nelson, J. Allan, and I. Carmichael (1985). Active rifting in southwestern Mexico: Manifestations of an incipient eastward spreading-ridge jump, *Geology* **13,** 54–57.

Madrigal, L. A., D. Núñez, F. J. Escalona-Alcázar, and F. J. Núñez-Cornú (2021). Crustal structure across the northern region of the Islas Marías Archipelago, *Front. Earth Sci.* **9,** doi: 10.3389/feart.2021.682206.

Manea, V. C., M. Manea, and L. Ferrari (2013). A geodynamical perspective on the subduction of Cocos and Rivera plates beneath Mexico and central America, *Tectonophysics* **609,** 56–81.

Marín-Mesa, T., F. J. Núñez-Cornú, and C. Suárez-Plascencia (2019). Analysis of the seismicity in the Jalisco block from June to December 2015, *Seismol. Res. Lett.* **90,** no. 5, 1767–1778, doi: 10.17885/0220190107.

McCaffrey, R., P. C. Zwick, Y. Bock, L. Prawirodirdjo, J. F. Genrich, C. W. Stevens, S. S. O. Puntodewo, and C. Subarya (2000). Strain partitioning during oblique plate convergence in northern Sumatra: Geodetic and seismologic constraints and numerical modeling, *J. Geophys. Res.* **105,** no. B12, 28,363–28,376.

Núñez-Cornú, F. J. (2011). Peligro Sísmico en el Bloque de Jalisco, México, *Rev. Geofís.* **23,** 199–229, doi: 10.5209/rev_FITE.2011.v23.36919 (in Spanish).

Núñez-Cornú, F. J., and C. Sánchez-Mora (1999). Stress field estimations for Colima volcano, Mexico, based on seismic data, *Bull. Volcanol.* **60,** 568–580.

Núñez-Cornú, D., J. A. Acosta-Hernández, F. J. Escalona-Alcázar, S. Pilia, F. J. Núñez-Cornú, and D. Córdoba (2021). The extended continental crust West of Islas Marías (Mexico), *Front. Earth Sci.* **9,** doi: 10.3389/feart.2021.666272.

Núñez-Cornú, D., F. J. Núñez-Cornú, F. J. Escalona-Alcazar, D. Córdoba, J. Y. López Ortiz, J. L. Carrillo de la Cruz, and J. J. Dañobeitia (2019). Seismic structure of southern Rivera plate and Jalisco block subduction zone, *Seismol. Res. Lett.* doi: 10.1785/0220180399.

Núñez-Cornú, F., G. Castellanos, F. A. Nava, G. Reyes-Dávila, B. Márquez, G. Calderón, A. Ramírez, O. Sánchez, Z. Jiménez, G. Ornelas, *et al.* (1994). Estructura de la corteza superior en la Región del Graben de Colima, *GEOS v 14 n 5*, 109 pp. (in Spanish).

Núñez-Cornú, F. J., D. Córdoba Barba, W. Bandy, J. J. Dañobeitia, J. E. Alarcón, D. Núñez, and C. Suárez-Plascencia (2021). The TsuJal amphibious seismic network: A passive-source seismic experiment in western Mexico, *Front. Earth Sci.* **9,** 738515, doi: 10.3389/feart.2021.738515.

Núñez-Cornú, F. J., D. Córdoba, J. J. Dañobeitia, W. L. Bandy, M. Ortiz Figueroa, R. Bartolomé, D. Núñez, A. Zamora-Camacho, J. M. Espindola, A. Castellon, *et al.* (2016). Geophysical studies across Rivera plate and Jalisco block, Mexico: TsuJal project, *Seismol. Res. Lett.* **87,** 59–72, doi: 10.1785/0220150144.

Núñez-Cornú, F. J., G. A. Reyes-Davila, M. Rutz Lopez, E. Trejo Gomez, M. A. Camarena-Garcia, and C. A. Ramirez-Vazquez (2004). The 2003 Armería, Mexico earthquake (M_w 7.4): Mainshock and early aftershocks, *Seismol. Res. Lett.* **75,** 734–743.

Núñez-Cornú, F. J., M. Rutz López, V. Márquez, C. Suarez Plascencia, and E. Trejo (2010). Using an enhanced dataset for reassessing the source region of the 2003 Armerıa, Mexico earthquake, México, *Pure Appl. Geophys.* **168,** 1293–1302.

Núñez-Cornú, F. J., M. Rutz-López, F. A. Nava, G. Reyes-Dávila, and C. Suárez-Plascencia (2002). Characteristics of the seismicity in the coast and north of Jalisco block, Mexico, *Phys. Earth Planet. In.* **132,** 141–155.

Núñez-Cornú, F. J., J. M. Sandoval, E. Alarcón, A. Gómez, C. Suárez-Plascencia, D. Núñez Escribano, E. Trejo-Gómez, O. Sanchez-Mariscal, J. Guadalupe Candelas Ortiz, and L. M. Zúñiga-Medina (2018). The Jalisco seismic accelerometric telemetric network (RESAJ), *Seismol. Res. Lett.* **89,** 363–372, doi: 10.1785/0220170157.

Pacheco, J. F., S. K. Singh, J. Domínguez, A. Hurtado, L. Quintanar, Z. Jiménez, J. Yamamoto, C. Gutiérrez, M. Santoyo, W. Bandy, *et al.* (1997). The October 9, 1995, Colima-Jalisco, Mexico earthquake (M_w 8): An aftershock study and a comparison of this earthquake with those of 1932, *Geophys. Res. Lett.* **24,** 2223–2226.

Pinzón, J., F. J. Núñez-Cornú, and C. A. Rowe (2016). Magma intrusion near Volcan Tancítaro: Evidence from seismic analysis, *Phys. Earth Planet. In.* **262,** 66–79, doi: 10.1016/j.pepi.2016.11.004.

Rutz-López, M., and F. J. Núñez-Cornú (2004). Sismotectónica del Norte y Oeste del Bloque de Jalisco usando datos sísmicos regionals, *GEOS* **24,** no. 1, 2–13 (in Spanish).

Rutz-López, M., F. J. Núñez-Cornú, and C. Suárez-Plascencia (2013). Study of seismic clusters at Bahía de Banderas region, Mexico, *Geofis. Int.* **52,** no. 1, 59–72.

Singh, S. K., A. Iglesias, D. Arroyo, X. Pérez-Campos, M. Ordaz, C. Mendoza, R. D. Corona-Fernández, L. Rivera, V. H. Espíndola, D. González-Ávila, *et al.* (2023) A seismological study of the Michoacán-Colima, Mexico, earthquake of 19 September 2022 (M_w 7.6), *Geofis. Int.* **62,** no. 2, 445–465, doi: 10.22201/igeof.2954436xe.2023.62.2.1453.

Singh, S. K., L. Ponce, and S. P. Nishenko (1985). The great Jalisco, Mexico, earthquakes of 1932: Subduction of the Rivera plate, *Bull. Seismol. Soc. Am.* **75,** 1301–1313.

Soto, G. L., J. F. Ni, S. P. Grand, E. Sandvol, R. W. Valenzuela, M. G. Speciale, J. G. González, and T. D. Reyes (2009). Mantle flow in the Rivera-Cocos subduction zone, *Geophys. J. Int.* **179,** 1004–1012.

Tinoco-Villa, M. E. (2015). Detección y Análisis de Enjambres Sísmicos en la Corteza Oceánica al Sur de las Islas Marías, *Master's Thesis*, Maestría en Ciencias en Geofísica, UdeG, 69 pp. (in Spanish).

Trejo-Gómez, E., M. Ortiz, and F. J. Núñez-Cornú (2015). Source Model of the October 9, 1995 Jalisco Colima as constrained by field survey reports, and on numerical simulation of the tsunami, *Geofis. Int.* **54,** no. 2, 149–159.

Urías-Espinosa, J., W. L. Bandy, C. A. Mortera-Gutiérrez, F. J. Núñez-Cornú, and N. C. Mitchell (2016). Multibeam bathymetric survey of the Ipala Submarine Canyon, Jalisco, Mexico (20°N): The southern boundary of the Banderas fore-arc block? *Tectonophysics* **671,** 249–263, doi: 10.1016/j.tecto.2015.12.029.

Watkins, W., C. H. Thurber, E. R. Abbott, and M. R. Brudzinski (2018). Local earthquake tomography of the Jalisco, Mexico region, *Tectonophysics* **724–725,** 51–64, doi: 10.1016/j.tecto.2018.01.002.

Wessel, P., J. F. Luis, L. Uieda, R. Scharroo, F. Wobbe, W. H. F. Smith, and D. Tian (2019). The Generic Mapping Tools version 6, *Geochem. Geophys. Geosys.* **20,** 5556–5564, doi: 10.1029/2019GC008515.

Yang, T., S. P. Grand, D. Wilson, M. Guzman-Speciale, J. M. Gómez-González, T. Dominguez-Reyes, and J. Ni (2009). Seismic structure beneath the Rivera subduction zone from finite-frequency seismic tomography, *J. Geophys Res.* **114,** no. B13, doi: 10.1029/2008JB005830.

Manuscript received 26 September 2023
Published online 29 April 2024